Inorganic Chemistry

Article

Cyclic Voltammetry of Th(IV) in the Room-Temperature Ionic Liquid [Me$_3$N^{n}Bu][N(SO$_2$CF$_3$)$_2$]

Anand I. Bhatt,*[†] Noel W. Duffy,[†,‡] David Collison,[§] Iain May,[||] and Robert G. Lewin[⊥]

School of Chemistry, Monash University, Clayton, Victoria 3800, Australia, School of Chemistry, The University of Manchester, Oxford Road, Manchester M13 9PL, U.K., Centre for Radiochemistry Research, School of Chemistry, The University of Manchester, Oxford Road, Manchester M13 9PL, U.K., and Nexia Solutions, BNFL, Sellafield, Seascale, Cumbria CA20 1PG, U.K.

A Th(IV) compound, [Th(TFSI)$_4$(HTFSI)]·2H$_2$O [where TFSI = N(SO$_2$CF$_3$)$_2$], has been synthesized and characterized using elemental analysis, thermogravimetric analysis, and vibrational spectroscopy. The analysis suggests that the TFSI anion coordinates to the metal center via the sulfonyl oxygens as well as provides evidence for the coordination of HTFSI. The voltammetric behavior of this compound has been studied in the room-temperature ionic liquid [Me$_3$N^{n}Bu][TFSI], and results show that Th(IV) is reduced to Th(0) in this ionic liquid in a single reduction step. Analysis of cyclic voltammograms shows that an insoluble product is being formed at the electrode surface, which is attributed to the formation of ThO$_2$ by reaction with water. The E^0 value for the reduction of Th(IV) to Th(0) has been determined to be −2.20 V (vs Fc$^+$/Fc; −1.80 V vs SHE). A comparison of this E^0 value with those obtained for Th(IV) reduction in a LiCl–KCl eutectic (400 °C), water, and nonaqueous solvents shows that the reduction in [Me$_3$N^{n}Bu][TFSI] is easier to accomplish than that in these other solvents.

Introduction

The electrochemical processing of spent nuclear fuels has been studied in high-temperature molten salts (e.g., equimolar NaCl−KCl) for a number of years. This process has been previously demonstrated on a near industrial scale in pilot plants at Argonne National Laboratories, Argonne West, Argonne, IL, which uses the LiCl−KCl eutectic (500 °C),[1] and at RIAR, Dimitrovgrad, Russia, which is based on NaCl−KCl melts (650 °C).[2] Although the technology can be used to separate both U and Pu from the rest of the fission products, the high temperatures of operation introduce problems in terms of plant design and corrosion from the use of highly reactive gases. Clearly, a switch to lower temperatures of operation would remove some of these problems. We have recently reported on the cyclic voltammetric (CV) behavior of Eu(III) in the low-temperature ionic salts of the general formula [Me$_4$X][TFSI] (where X = N, P, and As and TFSI = bis(trifluoromethanesulfonyl)amide, [N(SO$_2$CF$_3$)$_2$]$^−$, with melting points of ca. 135, 150, and 140 °C, respectively)[3] and have observed the Eu(II)/Eu(0) reduction in all three melts at 160 °C. Because the Eu(II)/Eu(0) standard reduction potential is more negative than that of either U(III)/U(0) or Pu(III)/Pu(0), then these melts have real potential for use in U and Pu electrorefining. However, it would be desirable to reduce the operating temperatures even further to room temperature. Recently, a number of publications[4−6] have reported on room-temperature ionic

* To whom correspondence should be addressed. E-mail: Anand.Bhatt@sci.monash.edu.au.

[†] Monash University.

[‡] Present address: CSIRO Energy Technology, Clayton South, Victoria 3169, Australia.

[§] School of Chemistry, The University of Manchester.

[||] Centre for Radiochemistry Research, School of Chemistry, The University of Manchester.

[⊥] Nexia Solutions, BNFL.

(1) McPheeters, C. C.; Pierce, R. D.; Mulcahey, T. P. *Prog. Nucl. Energy* **1997**, *31*, 175. Laidler, J. J.; Battles, J. E.; Miller, W. E.; Ackerman, J. P.; Carls, E. L. *Prog. Nucl. Energy* **1997**, *31*, 131.

(2) Bychkov, A. V.; Skiba, O. V. *Chemical Separation Technology and Related Methods of Nuclear Fuel Waste Management*; Kluwer Academic Publishers: Dordrecht, The Netherlands, 1999.

(3) Bhatt, A. I.; May, I.; Volkovich, V. A.; Hetherington, M. E.; Lewin, R. *Dalton Trans.* **2002**, 4532.

(4) Quinn, B. M.; Ding, Z.; Moulton, R.; Bard, A. J. *Langmuir* **2002**, *18*, 1734. MacFarlane, D. R.; Sun, J.; Golding, J.; Meakin, P.; Forsyth, M. *Electrochim. Acta* **2000**, *45*, 1271.

(5) Sun, J.; Forsyth, M.; MacFarlane, D. R. *J. Phys. Chem. B* **1998**, *102*, 8858.

(6) Murase, K.; Nitta, K.; Hirato, T.; Awakura, Y. *J. Appl. Electrochem.* **2001**, *31*, 1089.

liquids (RTILs) with electrochemical windows comparable to those observed for the [Me$_4$X][TFSI] (where X = N, P, and As) melts, e.g., [Et$_3$NOct][TFSI], for which a 5-V window was observed.[5] A recent study of Cs electrodeposition in the RTIL, [Bu$_3$NMe][TFSI],[7] suggests that, for some RTILs, the electrochemical window may have cathodic limits wider than those observed for molten salts, and therefore this would allow the RTILs to be used as lower temperature substitutes. Our long-term goal is the development of a U/Pu electrochemical separation process based on RTILs. For most of our initial studies, we are focusing on [Me$_3$N^{n}Bu][TFSI], chosen for its cathodic stability and ease of synthesis.[4] Our initial efforts were directed at nonradioactive analogues of the actinides, and we have recently reported on the reduction of La, Sm, and Eu to the zerovalent state in this RTIL.[8]

Th was chosen as an electrochemical actinide analogue for U and Pu because the Th(IV)/Th(0) standard reduction potential lies between those of U(III)/U(0) and Pu(III)/Pu(0) in aqueous media (−1.899 V compared to −1.789 and −2.031 V vs SHE[9]) and in a LiCl−KCl eutectic at 450 °C (−2.359 V compared to −2.218 and −2.535 V vs SHE,[10] respectively). In addition, the redox chemistry of Th is much simpler than that of U and Pu, where the III+, IV+, V+, and VI+ oxidation states are all readily accessible (see, for example, the work of Costa et al.[11]). Additionally, the similar ionic radii of Th(IV) vs U(IV) and Pu(IV) (94 pm compared to 89 and 86 pm, respectively) and similar coordination numbers allow a direct comparison between chemical speciation and diffusional parameters. The electrochemical behavior of Th has previously been investigated in molten salts[12] and in nonaqueous organic solvents;[13] however, to date, there have been no reports of electrochemical behavior of Th in ionic liquids. We here report on the CV behavior of a Th(IV)−TFSI complex in the RTIL, [Me$_3$N^{n}Bu][TFSI].

Experimental Section

All chemicals were reagent-grade, obtained commercially and used as supplied unless stated otherwise. Elemental analysis was performed using a CHNS-O EA1108 elemental analyzer and a Fisons Horizon elemental analyzer ICP-OES spectrometer.

Synthesis of [Me$_3$N^{n}Bu][TFSI]. Me$_2$N^{n}Bu (100 mL, 0.72 mol) was placed in a salt−ice bath at −17 °C. After 15 min, MeI (45 mL, 0.72 mol) was added dropwise over 1 h to form a white

precipitate of [Me$_3$N^{n}Bu]I. Et$_2$O (100 mL) was added to this precipitate with stirring, and to the resultant suspension was added 100 mL of H$_2$O to dissolve the solid. The aqueous phase was separated and H$_2$O removed in vacuo to form a white microcrystalline solid (yield of [Me$_3$N^{n}Bu]I = 127.8 g, 73.9%). Li[TFSI] (151.2 g, 0.53 mol) was dissolved in H$_2$O (150 mL) and added to a solution of [Me$_3$N^{n}Bu]I in H$_2$O (127.8 g, 0.53 mol in 200 mL) with stirring. The resultant pale-yellow-colored, water-immiscible, impure [Me$_3$N^{n}Bu][TFSI] liquid was separated and washed once with an aqueous solution of Na$_2$S$_2$O$_3$·5H$_2$O (5 g, 10 mL) and then washed with H$_2$O (200 mL). The purified [Me$_3$N^{n}Bu][TFSI] was then dried in vacuo at 110−130 °C to yield a colorless, clear ionic melt (yield = 181.6 g, 87.1%). Elem anal. Calcd: C, 27.27; H, 4.59; N, 7.07; S, 16.61. Found: C, 27.21; H, 4.78; N, 6.98; S, 16.18.

Synthesis of [Th(TFSI)$_4$(HTFSI)]·2H$_2$O. Th(NO$_3$)$_4$·6H$_2$O (0.25 g, 0.43 mmol) was dissolved in HNO$_3$ (1 mL, 1 M) and the resultant solution reacted with NaOH (0.14 g, 3.50 mmol in 2 mL of H$_2$O) with stirring to form a white precipitate of hydrated Th(OH)$_4$. The solid Th(OH)$_4$ was collected by centrifugation, suspended in 5 mL of H$_2$O, and reacted again with NaOH (0.14 g, 3.50 mmol in 2 mL of H$_2$O). The resultant solid was collected by centrifugation and dissolved in a solution of H[TFSI] (2.25 g, 8.00 mmol, 5 mL of H$_2$O) to form a clear solution. This solution was then heated at 80−90 °C for 5 h to produce a white, microcrystalline product, which was stored under Ar (near-quantitative yield). Elem anal. Calcd for [Th(TFSI)$_4$(HTFSI)]·2H$_2$O: C, 7.20; H, 0.30; N, 4.20; S, 19.21. Found: C, 7.60; H, 0.30; N, 4.39; S, 19.91.

Thermogravimetric Analysis (TGA). TGA was undertaken using a Mettler Toledo TGA/SDTA 851^e analyzer. The initial sample weight was recorded in air, and samples were heated in alumina crucibles from 25 to 900 °C at a rate of 5 °C min^{-1} in air. Decomposition points (T_{dec}) were obtained from the minimum of the first derivative of the curves. The sample (16.00 mg of [Th(TFSI)$_4$(HTFSI)]·2H$_2$O) was heated from 25 to 900 °C at a rate of 5 °C min^{-1}. TGA showed four decomposition steps at ca. 70, 160, 235, and 390 °C (mass loss of 0.46, 0.80, 2.77, and 9.63 mg, respectively). A final mass of 2.34 mg was recorded and attributed to the formation of ThO$_2$. Using the mass of ThO$_2$ measured at the end of the experiment, the initial mass of [Th(TFSI)$_4$(HTFSI)]·2H$_2$O present was calculated to be 14.79 mg. The discrepancy of 1.21 mg (between the measured and calculated masses) is attributed to absorbed water from the atmosphere and corresponds to 8 H$_2$O molecules per Th complex. The loss of this water corresponds to the first two decomposition steps at 70 °C (3 × H$_2$O) and 160 °C (5 × H$_2$O). The decomposition steps at 235 and 390 °C are assigned to the loss of coordinated TFSI and HTFSI to form ThO$_2$.

Vibrational Spectroscopy. Infrared spectra were obtained from a Bruker Equinox 55/Bruker FRA 106/5 spectrometer with a coherent 500-mW laser as solid samples (10 mg) using an ATR Golden Gate attachment. Raman spectra were recorded on the same instrument in the solid state (20-mg samples). Both the IR and Raman spectra were recorded with a resolution of 4 cm^{-1}. Solid-state ATR mid-IR and Raman spectra of [Th(TFSI)$_4$(HTFSI)]·2H$_2$O are given in the Supporting Information.

CV. All of the CV measurements were performed using an EG&G 273A potentiostat operated by model 250 Research Electrochemistry Software (M270), version 4.41. A typical three-electrode cell was employed comprising a large-surface-area Pt gauze counter electrode, Ag wire quasi reference electrode (QRE), and a GC disk working electrode (0.031 cm^2). All measurements were recorded at 25 °C inside a Faraday cage under an Ar atmosphere to minimize electrochemical noise and atmospheric O$_2$/H$_2$O interference. The solution was purged with Ar for at least 30

(7) Chen, P.-Y.; Hussey, C. L. *Electrochim. Acta* **2004**, *49*, 5125.
(8) Bhatt, A. I.; May, I.; Volkovich, V. A.; Collison, D.; Helliwell, M.; Polovov, I. B.; Lewin, R. G. *Inorg. Chem.* **2005**, *44*, 4934.
(9) *CRC Handbook of Chemistry and Physics*; Lide, D. R., Ed.; CRC Press: Boca Raton, FL, 1995.
(10) Plambeck, J. A. *J. Chem. Eng. Data* **1967**, *12*, 77.
(11) Anderson, C. J.; Choppin, G. R.; Prett, D. J.; Costa, D. A.; Smith, W.; *Radiochim. Acta* **1999**, *84*, 31. Hopkins, T. A.; Berg, J. M.; Costa, D. A.; Smith, W. H.; Dewey, H. J. *Inorg. Chem.* **2001**, *40*, 1820, Costa, D. A.; Smith, W. H.; Abney, K. D.; Oldham, W. J. *Plutonium Futures−The Science*; American Institute of Physics: Melville, NY, 2000.
(12) Martinot, L. *J. Radioanal. Nucl. Chem.* **1986**, *103*, 357. Martinot, L. *J. Less-Common Met.* **1989**, *147*, 73.
(13) (a) Martinot, L.; Licour, C.; Lopes, L. *J. Alloys Compd.* **1995**, *228*, 6. (b) Duyckaerts, G.; Degueldre, Cl. *J. Electroanal. Chem.* **1981**, *119*, 347. (c) Astheimer, L.; Schwochau, K. *J. Inorg. Nucl. Chem.* **1973**, *35*, 223.
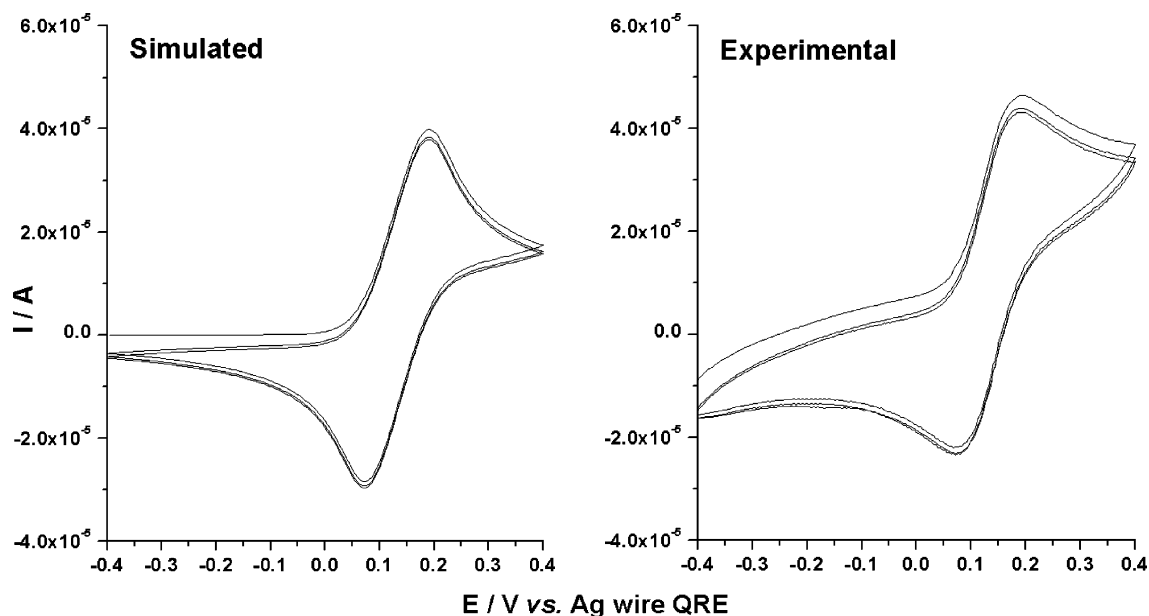
Figure 1. CV of Fc^+/Fc in $[Me_3N^nBu][TFSI]$ (0.06 mol L^{-1}) at a 10 mV s^{-1} scan rate and 25 °C and simulated CVs at 25 °C and 10 mV s^{-1}.
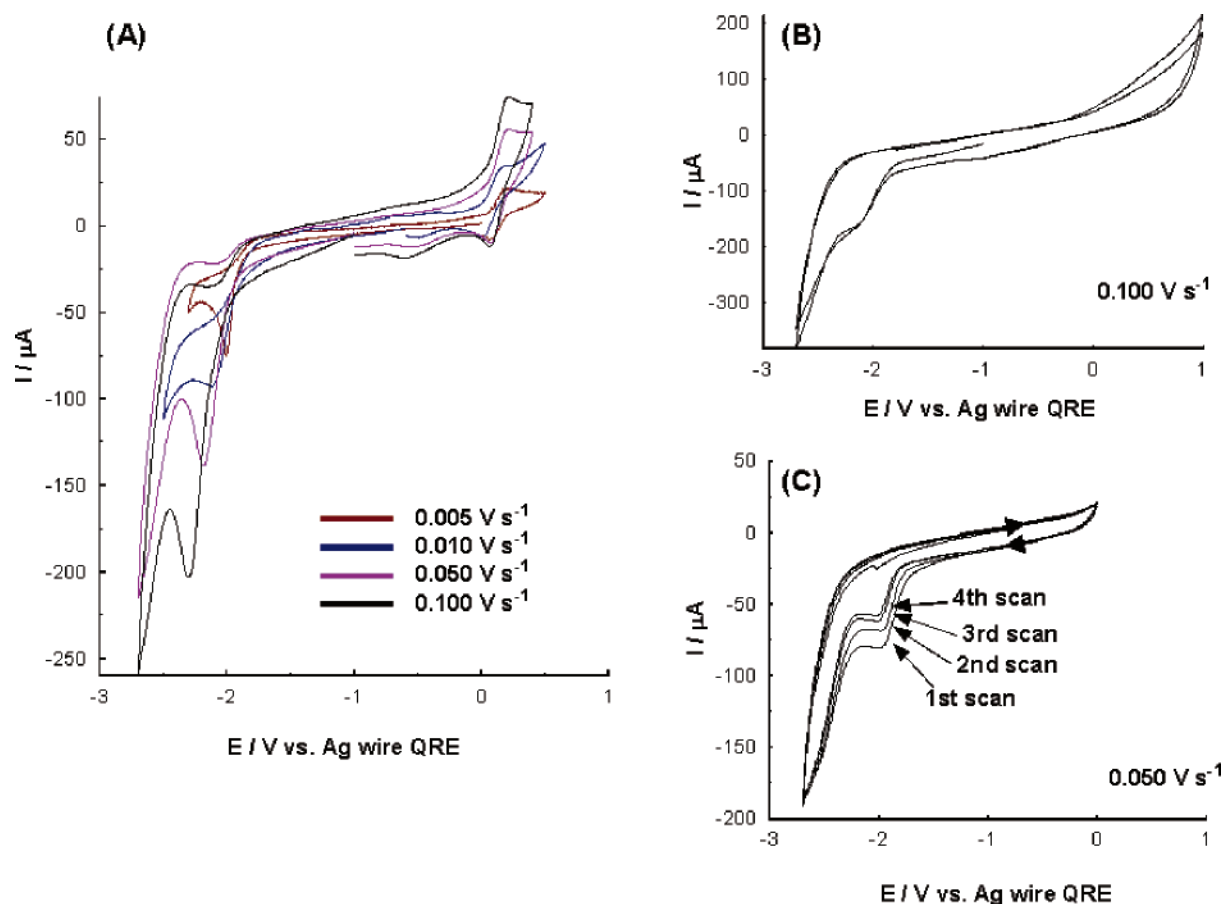
Figure 2. CVs of $H[Th(TFSI)_5] \cdot 2H_2O$ in $[Me_3N^nBu][TFSI]$ at 25 °C: (A) $H[Th(TFSI)_5] \cdot 2H_2O$ (0.05 mol L^{-1}) and ferrocene (0.06 mol L^{-1}) at varying scan rates; (B) $H[Th(TFSI)_5] \cdot 2H_2O$ (0.05 mol L^{-1}) in $[Me_3N^nBu][TFSI]$; (C) effect of multiple cycles around the Th(IV)/Th(0) reduction peak.

min prior to measurements and for 30 s between scans. The solution was kept under a blanket of Ar at all times. Prior to measurements, solution resistance was measured using the *iR* compensation option in the model 250 Research Electrochemistry Software, and all voltammograms were corrected by this value. CVs of ferrocene and $[Th(TFSI)_4(HTFSI)] \cdot 2H_2O$ (0.05 mol L^{-1}) in $[Me_3N^nBu][TFSI]$ were measured in the range of 0.005−0.5 V s^{-1} and are shown in

Figures 1 and 2. CVs were also recorded with added ferrocene (0.06 mol L^{-1}), and the Fc^+/Fc couple was used as an internal reference.[14]

Digital simulations of Fc^+/Fc in $[Me_3N^nBu][TFSI]$ were performed using DigiElch software, version 1.0 (copyright M. Rudolph,

(14) Noviandri, I.; Brown, K. N.; Fleming, D. S.; Gulyas, P. T.; Lay, P. A.; Masters, A. F.; Phillips, L. *J. Phys. Chem. B* **1999**, *103*, 6713.

2003), with a Fc concentration of 0.06 M and a diffusion coefficient of 8×10^{-9} cm s^{-1}. The best-fit voltammograms were corrected for iR drop with an uncompensated resistance (R_u) value of 650 Ω. DigiElch simulations of Th(IV) reduction in [Me$_3$N^{n}Bu][TFSI] were performed using an α value of 0.2,[8] and an electron-transfer rate constant (k_s) of 100 s^{-1}. The resulting voltammograms had a peak potential of -2.31 V and a peak current of 149 μA. The simulated voltammograms were corrected for iR drop with a R_u value of 650 Ω, calculated from the simulations of the Fc$^+$/Fc couple. The fitted E^0 value for the Th(IV) reduction in [Me$_3$N^{n}Bu]-[TFSI] was -2.20 V vs Fc$^+$/Fc (-1.80 V vs SHE).

Discussion

One of the reasons TFSI has been used as the anion in RTILs is because of its weakly coordinating properties. However, it is possible for TFSI to coordinate to metal centers, and a number of different coordination modes have been proposed. TFSI coordination to metal centers has previously been investigated using single-crystal X-ray diffraction. In [Cu(CO)$_2$TFSI], the Cu is coordinated to the central nitrogen,[15] and similarly in [Fe(CO)$_2$CpTFSI] (where Cp = C$_5$H$_5{}^-$), the Fe is coordinated to the central nitrogen.[16] For both [Mg(H$_2$O)$_6$][TFSI]$_2 \cdot$2H$_2$O[17] and [Cu(acac)(tmeda)]-[TFSI] (where acac = acetylacetonate and tmeda = tetramethylethylenediamine),[16] TFSI acts as a counterion to the {Mg(H$_2$O)$_6$}$^{2+}$ and [Cu(acac)(tmeda)]$^+$ cations. In [Cp$_2$Ti-(TFSI)$_2$], monodentate TFSI coordination via one of the sulfonyl oxygens has been observed,[16] and we have obtained similar results for [Ln(TFSI)$_3$(H$_2$O)$_3$] complexes (Ln = La, Sm, and Eu), where the Ln^{3+} center is coordinated to the TFSI anion via both sulfonyl oxygens.[8] In a recent study, Oldham et al. showed crystallographic evidence of TFSI coordination to transition-metal centers via both mono- and bidentate sulfonyl oxygen coordination as well as via the central N.[18]

The vibrational spectroscopy of [Th(TFSI)$_4$(HTFSI)]$\cdot$2H$_2$O shows bands due to TFSI[19] as well as bands that can be attributed to N$-$H[19] and O$-$H (from H$_2$O)[20] vibrations (see the Supporting Information). A comparison of the band positions to those of LiTFSI (where TFSI acts as a counterion)[21] and HTFSI (where TFSI coordinates through the nitrogen)[22] showed significant shifts in bands attributed to SO$_2$ (see the Supporting Information). A comparison of [Th-(TFSI)$_4$(HTFSI)]$\cdot$2H$_2$O band positions with those of [Ln-(TFSI)$_3$(H$_2$O)$_3$] complexes (Ln = La, Sm and Eu), where TFSI is known to coordinate via both sulfonyl oxygens, also showed similar shifts in band positions compared to LiTFSI

Table 1. Experimental and DigiElch Simulation Parameters for Fc$^+$/Fc and Th(IV)/Th(0) Reduction in [Me$_3$N^{n}Bu][TFSI] at 25 °C

Fc$^+$/Fc in [Me$_3$N^{n}Bu][TFSI]			Th(IV) in [Me$_3$N^{n}Bu][TFSI]		
parameter	exptl	simulated	parameter	exptl	simulated
$I_p^a \times 10^{-6}$ A	32	37	E_p^c/V vs Fc/Fc$^+$	-2.25	-2.22
$I_p^c \times 10^{-6}$ A	16	37	$I_p^c \times 10^{-6}$ A	153	149
E_p^a/V	0.189	0.191	scan rate/mV s^{-1}	100	100
E_p^c/V	0.072	0.073	E^0/V vs Fc/Fc$^+$		-2.20
scan rate/mV s^{-1}	10	10			

and HTFSI demonstrating that TFSI coordinates to the metal center. However, the spectra obtained for the Th complex are significantly different compared to the Ln complexes, with the major difference being the observation of the N$-$H vibration. Th(IV) is also known to have a high affinity for O donor ligands, and 10-coordinate complexes are common.

Therefore, we propose, on the basis of the vibrational spectroscopy results, that in H[Th(TFSI)$_5$]$\cdot$2H$_2$O the TFSI anions are coordinated to the Th center via the sulfonyl oxygens, as has been observed in [Cp$_2$Ti(TFSI)$_2$][16] and [La-(TFSI)$_3$(H$_2$O)$_3$].[8] Because of the higher coordination sphere of Th compared to Ti (10 coordinate compared to 6 coordinate), we believe that TFSI coordinates in a bidentate geometry similarly to the Ln(TFSI)$_3$(H$_2$O)$_3$ complexes. HTFSI is known to sublime at 60 °C; however, the TGA data indicate that HTFSI is lost at much higher temperatures. Thus, we conclude that HTFSI also coordinates to the Th center (as opposed to cocrystallization). In addition, the N$-$H modes observed in the IR/Raman spectra provide evidence for the coordination of HTFSI, as opposed to the formation of a monoprotic acid. However, it has not yet been possible to grow single crystals of the complex for a full structural analysis to confirm this prediction.

CV. CVs of Fc (0.06 M; Figure 1) in [Me$_3$N^{n}Bu][TFSI] show one cathodic peak and one anodic peak ($E_p^c = 0.072$ V, $E_p^a = 0.189$ V vs Ag wire QRE at a 10 mV s^{-1} scan rate). The midpoint potential was calculated to be 0.131 V (vs Ag wire QRE). The apparent number of electrons transferred was determined using $E_{pk/2} - E_{pk} = 2.2RT/nF$ (assuming a diffusion-controlled mechanism, where E_{pk} is the peak potential, $E_{pk/2}$ is the peak potential at half-intensity, and other symbols have their usual meanings)[23] and found to be 0.8 electrons at a 5 mV s^{-1} scan rate. The difference between the calculated and expected number of electrons (1.0 for the Fc/Fc$^+$ couple) is attributed to high solution resistance, as is evident by the peak$-$peak separation of ca. 117 mV (the expected separation is 58 mV for a one-electron reversible system at 20 °C). The amount of solution resistance present was calculated by simulating the experimental CVs using DigiElch. Figure 1 shows the experimental and simulated voltammograms, and the experimental parameters are summarized in Table 1. The best-fit simulation was achieved using a R_u value of 650 Ω, and this value explains the large peak$-$peak separations observed in the experimental CVs.

(15) Polyakov, O. G.; Ivanova, S. M.; Gaudinski, C. M.; Miller, S. M.; Anderson, O. P.; Strauss, S. H. *Organometallics* **1999**, *18*, 3769.

(16) Oldham, W. J.; Williams, D. B. *Proc. Electrochem. Soc.* **2002**, *19*, 983.

(17) Haas, A.; Klare, C.; Betz, P.; Bruckmann, J.; Kruger, C.; Tsay, Y. H.; Aubke, F. *Inorg. Chem.* **1996**, *35*, 1918.

(18) Williams, D. B.; Stoll, M. E.; Scott, B. L.; Costa, D. A.; Oldham, W. J. *Chem. Commun.* **2005**, 1438.

(19) Rey, I.; Johansson, P.; Lindgren, J.; Lassègues, J. C.; Grondin, J.; Servant, L. *J. Phys. Chem. A* **1998**, *102*, 3249. Rey, I.; Lassègues, J. C.; Grondin, J.; Servant, L. *Electrochim. Acta* **1998**, *43*, 1505.

(20) Saito, A.; Choppin, G. R. *Inorg. Chem.* **1991**, *30*, 4563.

(21) Nowinski, J. L.; Lightfoot, P.; Bruce, P. G. *J. Mater. Chem.* **1994**, *4*, 1579.

(22) Žák, Z.; Rùžička, A.; Michot, Ch. *Z. Kristallogr.* **1998**, *213*, 217.

(23) Bard, A. J.; Faulkner, L. R. *Electrochemical Methods: Fundamentals and Applications*; John Wiley & Sons Inc.: New York, 2001.

CVs of $[Th(TFSI)_4(HTFSI)]\cdot 2H_2O$ in $[Me_3N^nBu][TFSI]$ (0.05 M; Figure 2)[24] show a single, irreversible cathodic peak at ca. -2.15 V. On the basis of the known electrochemical behavior of Th in nonaqueous solvents, the cathodic peak at -2.15 V is likely to be due to either the Th(IV)/Th(0) or Th(IV)/Th(II) processes.[13] The addition of ferrocene (0.06 M) as an internal standard confirmed the former process because the cathodic peak position ($E_p^c = -2.29$ V vs Fc/Fc$^+$) is close to that of the standard reduction potential of the Th(IV)/Th(0) process compared to ferrocene ($E^0 = -2.30$ V vs Fc$^+$/Fc).[9] This result indicates that the Th(IV)/Th(0) process is the most likely in this solvent and is consistent with Th(IV) reduction in dimethyl sulfoxide (DMSO)[13a,b] and in a molten LiCl$-$KCl eutectic.[12]

It would be expected for the reduction of Th(IV) ions to Th(0) metal that the voltammetry would show plating/stripping behavior. However, there is an absence of a stripping or anodic peak in the voltammograms obtained. A previous study of the Th(IV) electrochemistry in DMSO has shown the formation of ThO_2 upon reduction of Th(IV) to Th metal.[13a] Additionally, a study of the La(III) electrochemistry in a chloroaluminate RTIL showed similar behavior, i.e., formation of an oxide phase after a three-electron reduction.[25] Both TGA and vibrational spectroscopy suggest the presence of water in the Th complex; therefore, it is hypothesized that Th(IV) is electrochemically reduced to a metallic state and reacts chemically with the H_2O present to yield ThO_2. It should be noted that no hydrogen evolution was observed at the working electrode during the voltammetry. Multiple cycles around this region showed a decrease in the current intensity for the reduction peak, as would be expected for the formation of a nonconducting oxide layer (Figure 2C). It is known for an irreversibly adsorbed species on the electrode surface that the peak potential is dependent on the scan rate and is described by the following relationship:[23]

$$E_p = E^0 + \frac{RT}{\alpha nF}\ln\left(\frac{RT}{\alpha nF}\frac{k^0}{\nu}\right)$$

where α = mass-transfer coefficient, n = number of electrons transferred, F = Faraday's constant, R = gas constant, T = temperature, k^0 = electron-transfer rate constant, and ν = scan rate.

A plot of E_p vs $\ln(1/\nu)$ shows a linear relationship (Figure 3) and suggests that the reduction of Th(IV) and adsorption of Th(0) onto the electrode and the subsequent formation of an oxide is a plausible explanation of the experimental data. However, further investigation into the electrode mechanism needs to be conducted before a full mechanism is assigned for the reduction of Th(IV) in this solvent system.
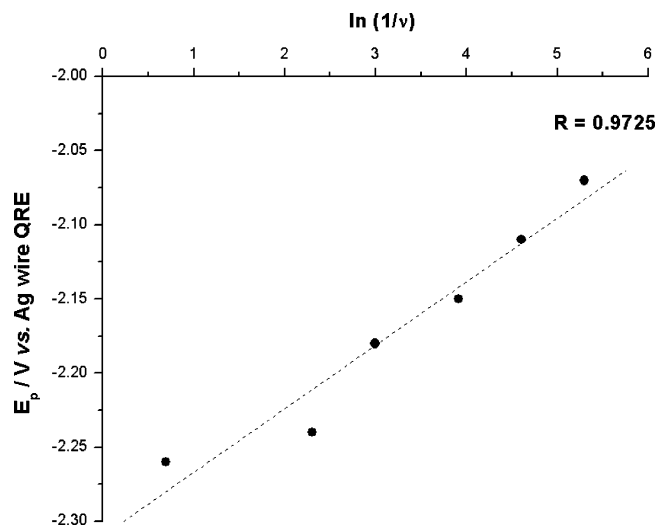

Figure 3. Plot of E_p vs $\ln(1/\nu)$ for the Th(IV) reduction peak from 5 to 500 mV s^{-1}.

The E^0 value can be obtained from the intercept of the plot of E_p vs $\ln(1/\nu)$ (Figure 3). However, determination of the E^0 value using this method, for this experimental data set, is unreliable because neither α nor k^0 is known for Th(IV) reduction in this ionic liquid. Nevertheless, an apparent value, E_{app}^0, of -2.31 V vs Fc$^+$/Fc has been calculated. A more reliable E^0 value has been calculated for the Th(IV) reduction in $[Me_3^nNBu][TFSI]$ using DigiElch simulations, and Figure 4 shows the simulated voltammograms coplotted with the experimental data, with experimental parameters summarized in Table 1. The best-fit simulation gave an E^0 value of -2.20 V vs Fc$^+$/Fc (-1.80 V vs SHE). Table 1 shows the $E_{1/2}$ values for the Th(IV)/Th(0) reduction in a LiCl$-$KCl eutectic at 450 °C[26] and the calculated value in an aqueous solution.[27] A comparison of these standard potentials (Table 2) shows that in $[Me_3N^nBu][TFSI]$ the reduction of Th is easier to accomplish than in both a LiCl$-$KCl eutectic and aqueous media, as is evident by the significantly more positive value obtained. This positive shift in the E^0 value shows that in this ionic liquid the TFSI anion is a poor ligand for the Th(IV) center, thus facilitating the reduction to the zerovalent state. By comparison with both a LiCl$-$KCl eutectic and water, ligands with strong affinity for highly charged cations (Cl$^-$ and H_2O) are present and can stabilize the Th(IV) center, thereby positively shifting the relative E^0 position compared to the ionic liquid.

Unfortunately, because of the lack of experimental data in nonaqueous solvents, comparisons of the E^0 values are more complex because they have not been reported previously. An approximate comparison of the $E_{1/2}$ values obtained in nonaqueous solvents using polarography (Table 1) can be performed.[27] These results suggest that the E^0 value is also more positive than those obtained in nonaqueous

(24) Figure 2C was previously published as a conference proceedings: Bhatt, A. I.; Kinoshita, H.; Koster, A. L.; May, I.; Sharrad, C.; Steele, H. M.; Volkovich, V. A.; Fox, O. D.; Jones, C. J.; Lewin, B. G.; Charnock, J. M.; Hennig, C. *Abstracts of Papers of the American Chemical Society*; 227th ACS National Meeting, Anaheim, CA, Mar 28$-$Apr 1, 2004; American Chemical Society: Washington, DC, 2004.
(25) Tsuda, T.; Ito, Y. *Proc. Electrochem. Soc.* **2000**, *99-41* (Molten Salts XII), 100.
(26) Sakamura, Y.; Hijikata, T.; Kinoshita, K.; Inoue, T.; Storvick, T. S.; Krueger, C. L.; Roy, J. J.; Grimmett, D. L.; Fusselman, S. P.; Gay, R. L. *J. Alloys Compd.* **1998**, *271$-$273*, 592.
(27) Martinot, L. The Actinides. In *Encyclopedia of Electrochemistry of the Elements*; Bard, A. J., Ed.; Marcel Dekker: New York, 1978; Vol. 7.
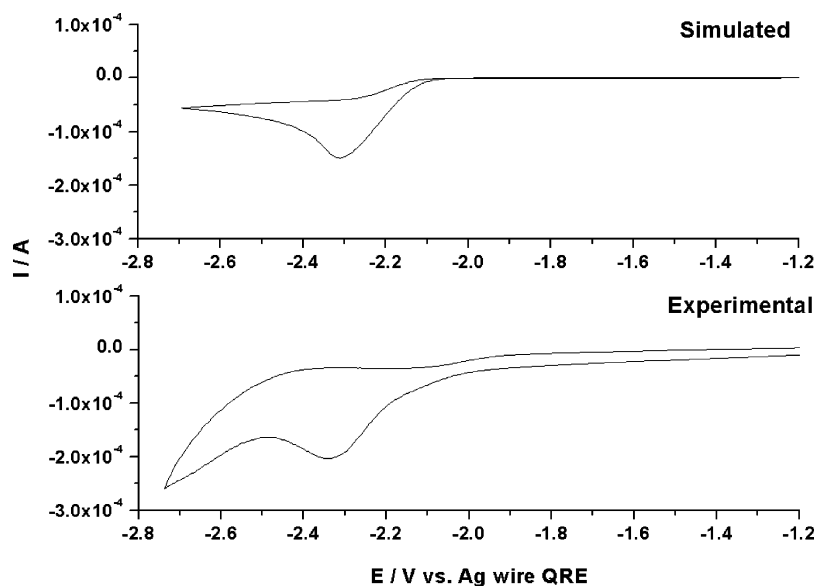
Figure 4. Simulated and experimental CVs of the Th(IV)/Th(0) reduction in [Me$_3$N^{n}Bu][TFSI] at 25 °C and 100 mV s^{-1}.

Table 2. Comparison of the E^0 Values (V) for the Th(IV)/Th(0) Reduction in [Me$_3$N^{n}Bu][TFSI] at 25 °C with Aqueous and Nonaqueous Solvents and a LiCl—KCl Eutectic

solvent	E^0 vs SHE	$E_{1/2}$ vs SHE	reference
[Me$_3$N^{n}Bu][TFSI] at 25 °C	−1.80		this work
LiCl—KCl eutectic at 450 °C	−2.359		32
aqueous solution at 25 °C^a	−1.899		33
propylene carbonate (0.1 M Et$_4$NClO$_4$)		−1.85	33
dimethylacetamide (0.1 M Et$_4$NClO$_4$)		−2.14	33
DMSO (0.1 M Et$_4$NClO$_4$)		−1.88	33

^{a} Calculated value for 1 M HClO$_4$.

solvents, suggesting that the TFSI anion may also be a poorer coordinating ligand for Th(IV) than nonaqueous solvents.

Conclusions

An [Th(TFSI)$_4$(HTFSI)]·2H$_2$O complex has been synthesized and characterized using vibrational spectroscopy and TGA. The analysis suggests that the Th(IV) center is 10-coordinate with four TFSI$^-$ ligands and HTFSI filling the coordination sphere. The vibrational spectroscopy suggests that TFSI$^-$ coordinates via both sulfonyl oxygens in a bidentate geometry.

The reduction of Th(IV) to the zerovalent state has been observed and investigated using CV in the RTIL [Me$_3$N^n-Bu][TFSI], and the E^0 has been determined to be −2.20 V (vs Fc$^+$/Fc; −1.80 vs SHE). The voltammetric analysis suggests that this reduction process is complicated by the subsequent formation of an oxide phase on the electrode surface. Although further research is required to understand

(and inhibit) this oxide formation reaction, the data obtained do show that Th can be reduced to the zerovalent state in this RTIL. A comparison of the reduction potentials with those in molten salts, aqueous solutions, and organic solvents shows that the Th reduction is easier to accomplish in the RTIL [Me$_3$N^{n}Bu][TFSI] than in molten salts and nonaqueous solvents. These results show the first evidence for electrochemical behavior of Th in RTILs, and future studies should focus on the elimination of moisture from the Th(IV) starting material, electrodeposition and characterization of a metallic phase, and investigations on the effect of different ionic liquids on the Th reduction process.

Overall the results show that Th(IV) reduction to the zerovalent state in [Me$_3$N^{n}Bu][TFSI] is possible, and therefore presumably reduction of other less electropositive actinides, e.g., U, may also be possible. In addition, the results also suggest that this RTIL can reduce species with very negative reduction potentials and may be of use for other metal reduction processes.

Supporting Information Available: Solid-state ATR mid-IR and Raman bands and spectra of [Th(TFSI)$_4$(HTFSI)]·2H$_2$O. This material is available free of charge via the Internet at http://pubs.acs.org.

IC051750I